THE ASTROPHYSICAL JOURNAL, 450:712–721, 1995 September 10

AGES FOR GLOBULAR CLUSTERS WITH PREDOMINANTLY RED HORIZONTAL BRANCHES

ATA SARAJEDINI
Kitt Peak National Observatory, National Optical Astronomy Observatories[1], P.O. Box 26732, Tucson, AZ 85726; ata@noao.edu
AND
YOUNG-WOOK LEE AND DONG-HAN LEE
Yonsei University Observatory, Seoul 120-749, Korea; ywlee@galaxy.yonsei.ac.kr
Received 1995 February 6; accepted 1995 March 21

ABSTRACT

We have used the $B-V$ color difference (d_{B-V}) between the horizontal branch (HB) and the red giant branch to explore the ages of globular clusters with red HB morphologies. Of these, 14 are Galactic, one belongs to the Large Magellanic Cloud (ESO 121–SC 03), and another to the Small Magellanic Cloud (Lindsay 1). Our observed values of d_{B-V} for these clusters are compared with theoretical values derived by constructing synthetic red HB models with a range of metallicities and ages. Based on ages determined via this comparison and main-sequence turnoff photometry for a subset of our clusters, we conclude that the usefulness of d_{B-V} as an age indicator seriously diminishes for clusters with [Fe/H] > -0.7. Furthermore, the Galactic globular clusters with [Fe/H] ≤ -0.7 and red HBs have a weighted mean age of $\langle \text{age} \rangle = 11.6 \pm 0.3$ Gyr, where the uncertainty is the standard error of the weighted mean. In contrast, from the work of Chaboyer, Sarajedini, and Demarque, clusters with HB morphologies bluer than those considered herein have $\langle \text{age} \rangle = 14.0 \pm 0.3$ Gyr, leading to the conclusion that the red HB clusters are younger than the remaining clusters by 2.4 ± 0.4 Gyr. This, and other evidence presented here, reinforces the conclusion of previous investigators that age is the second parameter, which, in addition to metal abundance, governs the morphology of the HB.

Subject headings: globular clusters: general — Hertzsprung-Russell diagram — Magellanic Clouds — stars: evolution

1. INTRODUCTION

The determination of star cluster ages has traditionally required the use of photometry reaching fainter than the main-sequence turnoff. However, this is not necessarily true in light of the latest results concerning the "second parameter" effect among Galactic globular clusters. A number of authors (Lee, Demarque, & Zinn 1994, and references therein; Zinn 1993; Chaboyer, Sarajedini, & Demarque 1992, 1995) have shown that, at intermediate metallicities, clusters with blue horizontal branch (HB) morphologies are, in the mean, older than those with relatively redder HBs. Thus, *in considering the Galactic globular cluster system as a whole*, the primary parameters affecting the morphology of the HB are metal abundance (the first parameter) and age (the second parameter).

A natural extension of this conclusion is to consider the mean color of the HB as an age indicator. This is especially important for clusters with *purely* red HBs because morphology indices based on the numbers of stars in various regions of the HB (see below) saturate and become insensitive to possible age variations between clusters with purely red HBs. On the other hand, the mean color of the red HB does have one obvious drawback. In order to make effective comparisons between clusters, the relative reddenings must be known. To circumvent this problem, it is possible to use the color difference between the HB and the red giant branch (RGB) as an age indicator. Thus, this quantity is independent of reddening and distance.

Hatzidimitriou (1991) used the $B-R$ color difference (d_{B-R}) to study the ages of open and globular clusters. The majority of Hatzidimitriou's clusters were originally observed in $B-V$, which she converted to $B-R$ using the calibration provided by the Revised Yale Isochrones (Green, Demarque, & King 1987). In addition, her calibration of d_{B-R} in terms of age is an empirical one relying on clusters with known metallicities and ages.

In contrast to Hatzidimitriou's approach, our aim in this work is to construct a theoretical calibration of d_{B-V} in terms of age and metallicity. In this way, we avoid the conversion of $B-V$ colors to $B-R$, and we can fully explore the dependence, or lack thereof, of d_{B-V} on metal abundance. Thus, in the next section, we describe the observational database to be used in our analysis. Section 3 discusses the theoretical models on which our d_{B-V}: age calibration is based, and § 4 presents the derived ages for clusters in our sample. There is main-sequence photometry for some of our clusters, and these data are analyzed in § 5. Finally, a discussion of our results is presented in § 6 and the conclusions in § 7.

2. OBSERVATIONAL DATA

The observational database used in this study consists of photometric and abundance parameters for a number of globular clusters with predominantly red HBs. They were selected from the compilation of Lee et al. (1994) based upon their $(B-R)/(B+V+R)$ index. This quantity was devised by Lee (1990) and is composed of the numbers of stars on the blue (B) and red (R) portions of the HB, as well as the numbers of RR Lyrae variables (V). It has a value of -1 for clusters with

[1] NOAO is operated by the Association of Universities for Research in Astronomy, Inc., under contract with the National Science Foundation.

completely red HBs and +1 for those with blue HBs. The majority of the clusters in our sample have $(B-R)/(B+V+R) = -1.0$. The remaining clusters are NGC 362 $[(B-R)/(B+V+R) = -0.87]$ and Rup 106 $[(B-R)/(B+V+R) = -0.82]$. Table 1 lists the relevant observational quantities for each cluster along with the associated literature references. The techniques used to derive these observational quantities are described in the following subsections.

2.1. *Horizontal Branch*

We measure two quantities of the HB: the mean magnitude, V(HB), and the mean color, $\langle(B-V)_{HB}\rangle$. Except for NGC 362, Rup 106, and perhaps AM-1, the magnitude and color ranges over which these values should be measured are evident by inspection of the CMDs. Figure 1 shows the CMDs of these clusters with the red HB enclosed by a rectangle. The solid line is our fit to the RGB stars and will be discussed in the next section. Each rectangle is 0.15 mag in $B-V$ and 0.4 mag in V. The mean HB magnitudes and colors are then computed using the stars in these rectangles. Since the HBs of NGC 362 and Rup 106 extend over a significant range in color and magnitude, we apply a different technique to these two clusters. Figures 2 and 3 illustrate our approach, which involves constructing color and magnitude histograms of the HB stars and fitting Gaussian profiles to the peaks, thereby measuring V(HB) and $\langle(B-V)_{HB}\rangle$. In the CMD shown in each figure, the filled circles denote the stars used in the construction of the histograms. The error attributed to V(HB) is calculated by adding, in quadrature, the standard error of the mean (s.e.m.) and an estimated uncertainty in the photometric zero point of $\pm$ 0.02 mag. In the case of $\langle(B-V)_{HB}\rangle$, Table 1 lists only the s.e.m. for reasons that will become clearer below. In the case of AM-1, the HB appears to be somewhat extended in color; however, to be consistent with the other $(B-R)/(B+V+R) = -1.0$ clusters in our sample, we have placed our standard HB rectangle around the most obvious clump of stars on the HB and used these stars to compute V(HB) and $\langle(B-V)_{HB}\rangle$. Furthermore, a comparison of the HB-rectangle locations of Eridanus, Pal 14, and AM −1 supports this choice.

A number of individual clusters deserve further comment. For C 0422−213 (hereafter Eridanus), we have used the photometry of Da Costa (1985) to measure V(HB) and $\langle(B-V)_{HB}\rangle$, but we note that the data of Ortolani & Gratton (1989), plotted as open circles in Figure 1, yield very similar results. For Pal 14, the filled circles show the photometry of Holland & Harris (1992), which has been used to measure $\langle(B-V)_{HB}\rangle$. The open circles are data obtained by one of us (A. S.) under nonphotometric conditions using the 4 m telescope at Kitt Peak National Observatory. The reduction of the resulting CCD images was identical to the study of Sarajedini (1994). The instrumental magnitudes have been calibrated to the standard system using the Holland & Harris (1992) data.

2.2. *Red Giant Branch*

The color of the red giant branch at the level of the HB $[(B-V)_g]$ is determined using the same technique as Sarajedini & Norris (1994). For all stars redder than the reddest extent of the HB box, and brighter than $\approx$ 0.5 mag below the HB, we fit a low-order polynomial of the form $B-V = f(V)$. Any points located more than 2 σ in $B-V$ away from this relation are excluded and the fit redone. We iterate until the number of points excluded is zero. The resulting fits are plotted in the panels of Figure 1; Figures 2 and 3 show the fits for NGC 362 and Rup 106, respectively. Once the RGB has been fitted with a polynomial, it is a simple matter to read the value of $(B-V)_g$ from this relation. The error in each value of $(B-V)_g$ is computed by considering only stars used in the RGB fit. The standard error in $B-V$ of these stars from the fit is the adopted error and is listed in Table 1. The uncertainty in the photometric zero point has been ignored when estimating the errors in $(B-V)_g$ and $\langle(B-V)_{HB}\rangle$. This is because these two quantities are subtracted to form d_{B-V} whose error (last column of Table 1) is composed of the s.e.m. of $\langle(B-V)_{HB}\rangle$ and the s.e.m. of $(B-V)_g$ added in quadrature.

Several individual clusters in Figure 1 deserve further comment. For Eridanus, the dashed line represents the fiducial

TABLE 1

OBSERVATIONAL DATA

Name	CMD Reference	V(HB)	σ	[Fe/H]	σ	Reference	$\langle(B-V)_{HB}\rangle$	s.e.m. (mmag)	$(B-V)_g$	s.e.m. (mmag)	d_{B-V}	σ
NGC 5927	1	16.60	0.02	−0.41	0.08	1	1.320	6.0	1.473	4.9	0.153	7.7
NGC 6496	1	16.47	0.02	−0.45	0.07	1	1.060	4.7	1.217	4.0	0.157	6.2
NGC 6352	1	15.28	0.02	−0.51	0.08	2	1.057	4.8	1.204	3.3	0.147	5.8
NGC 6624	1	16.11	0.02	−0.51	0.07	1	1.089	6.2	1.269	3.8	0.180	7.3
NGC 6637	1	16.00	0.02	−0.58	0.07	1	0.919	3.7	1.099	2.1	0.180	4.3
NGC 6366	2	15.60	0.03	−0.67	0.07	3	1.579	5.0	1.727	4.1	0.148	6.5
47 Tuc	1, 3	14.11	0.03	−0.71	0.08	2	0.800	11.0	0.996	1.6	0.196	11.0
ESO 121−SC 03	4	18.96	0.02	−0.93	0.10	4	0.792	4.4	0.937	7.4	0.145	8.6
Pal 12	5	17.10	0.02	−1.06	0.12	5	0.752	6.5	0.924	2.7	0.172	7.0
Lindsay 1	6	19.34	0.02	−1.10	0.10	6	0.752	4.1	0.904	2.2	0.152	4.7
NGC 362	7	15.44	0.02	−1.27	0.07	2	0.624	4.7	0.862	3.1	0.238	5.6
Pal 4	8	20.65	0.03	−1.28	0.20	7	0.566	6.2	0.795	3.0	0.229	6.9
Eridanus	9, 10	20.24	0.02	−1.41	0.11	8	0.675	14.0	0.868	7.3	0.193	15.8
Pal 14	11, 12	20.04	0.02	−1.60	0.18	7	0.619	7.2	0.853	3.2	0.234	7.9
Am-1	13	20.93	0.03	−1.7	0.2	9	0.590	9.2	0.787	6.8	0.197	11.4
Rup 106	14	17.80	0.02	−1.69	0.05	10	0.643	10.6	0.910	2.9	0.267	11.0

CMD REFERENCES.—(1) Sarajedini & Norris 1994; (2) Harris 1993; (3) Hesser et al. 1987; (4) Mateo et al. 1986; (5) Stetson et al. 1989; (6) Olszewski et al. 1987; (7) Harris 1982; (8) Christian & Heasley 1986; (9) Da Costa 1985; (10) Ortolani & Gratton 1989; (11) Holland & Harris 1992; (12) This paper; (13) Madore & Freedman 1989; (14) Buonanno et al. 1993.

[Fe/H] REFERENCES.—(1) Sarajedini & Norris 1994; (2) Zinn & West 1984; (3) Da Costa & Armandroff 1995; (4) Olszewski et al. 1991; (5) Da Costa & Armandroff 1990; (6) Da Costa & Hatzidimitriou 1995; (7) Armandroff et al. 1992; (8) Armandroff & Da Costa 1991; (9) Suntzeff et al. 1985; (10) Da Costa et al. 1992.

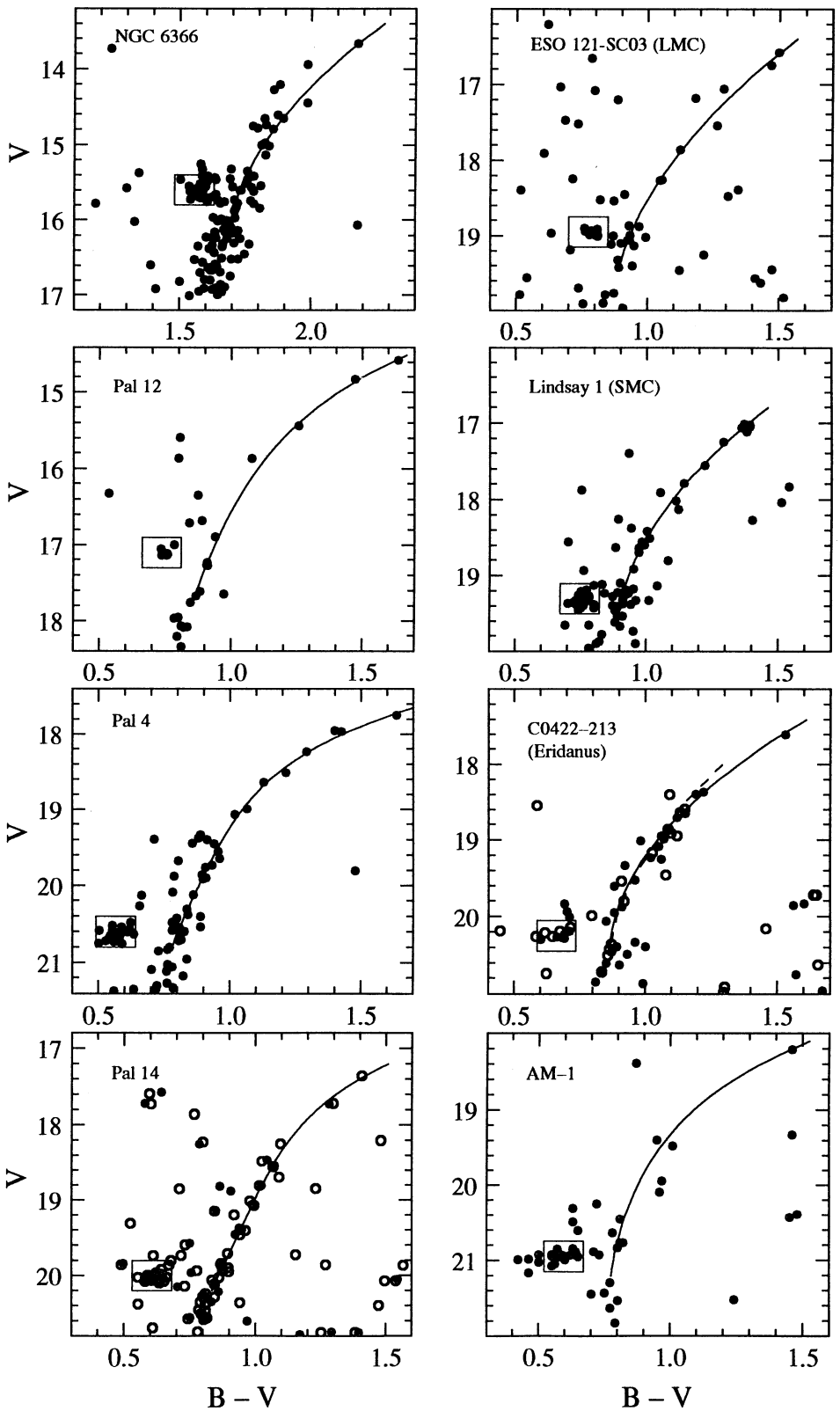

FIG. 1.—Color–magnitude diagrams for eight clusters in our sample that possess completely red horizontal branches [i.e., $(B-R)/(B+V+R) = -1$]. The solid lines have been fitted to the red giant branches (RGBs) to facilitate the measurement of the RGB color at the level of the horizontal branch. The boxes placed in each panel enclose the stars used in the calculation of $\langle B-V\rangle_{HB}$ and $\langle M_V(\mathrm{HB})\rangle$.

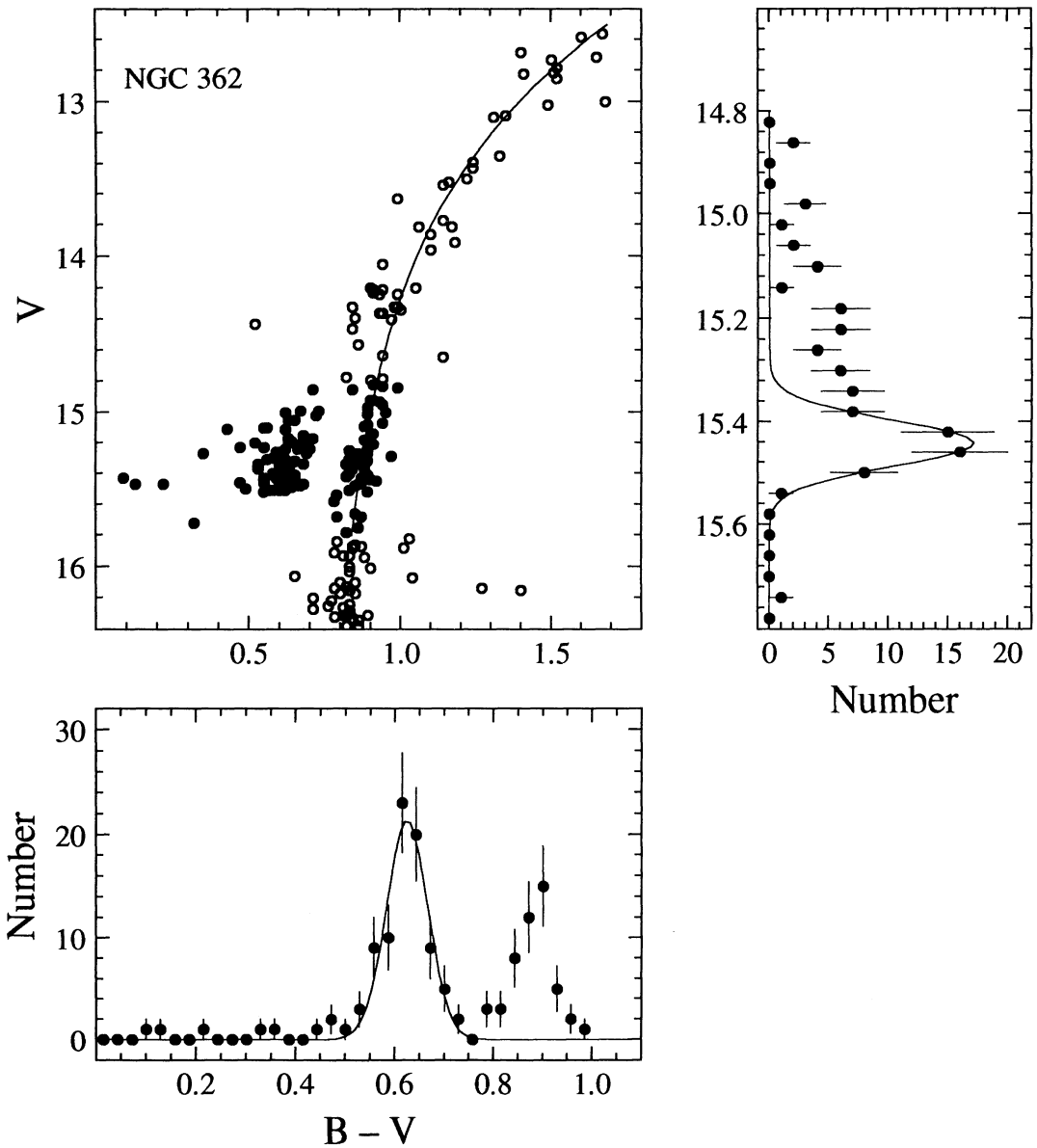

FIG. 2.—Color–magnitude diagram for NGC 362 using the photometry of Harris (1982). The relevant peaks in the color (*lower panel*) and magnitude (*right panel*) histograms for the filled circles have been fitted with Gaussians in order to measure the values of $\langle B-V\rangle_{HB}$ and $\langle M_V(HB)\rangle$.

sequence tabulated by Ortolani & Gratton (1989) and illustrates the close agreement between this fiducial and our RGB fit. In the case of Pal 14, it is important to note that, while the HB photometry of Holland & Harris (1992) was used to measure $\langle(B-V)_{HB}\rangle$, the RGB data obtained in the present study were fitted by a polynomial in order to derive $(B-V)_g$. This was done because the latter data set better samples the RGB shape. This mixing of photometry should not pose a problem because both data sets have been calibrated to the same scale. The RGB of AM-1 is quite sparse, and one could argue that this introduces significant uncertainty into the method used to determine $(B-V)_g$ (i.e., the iterative polynomial fit). However, by comparing the RGB of AM-1 with those of NGC 6535 (Sarajedini 1994), NGC 1904 (Ferraro et al. 1992), and NGC 362, which bracket AM-1 in metallicity (see below), we have confirmed our derived $(B-V)_g$ for AM-1.

2.3. *Metallicity*

The sources for the cluster metallicities are given in Table 1. Three of the four of the most metal-rich clusters have metal abundances taken from the recent CCD photometric study of Sarajedini & Norris (1994). Their abundance values agree with those of Zinn & West (1984) but frequently have smaller formal errors. Many of the clusters in Table 1 such as NGC 6366, ESO 121–SC 03, Lindsay 1, Pal 4, Eridanus, Pal 14, and Rup 106 have metal abundances derived using the calcium triplet lines. Note that, because Olszewski, Schommer, & Aaronson (1991) do not quote a formal error for the metallicity of ESO 121–SC 03, we have applied the small-sample statistical formulae of Keeping (1962, p. 202) to their measured abundances for four stars. The metallicities of NGC 6352 (see also Sarajedini & Norris 1994), 47 Tuc, and NGC 362 are taken from Zinn &

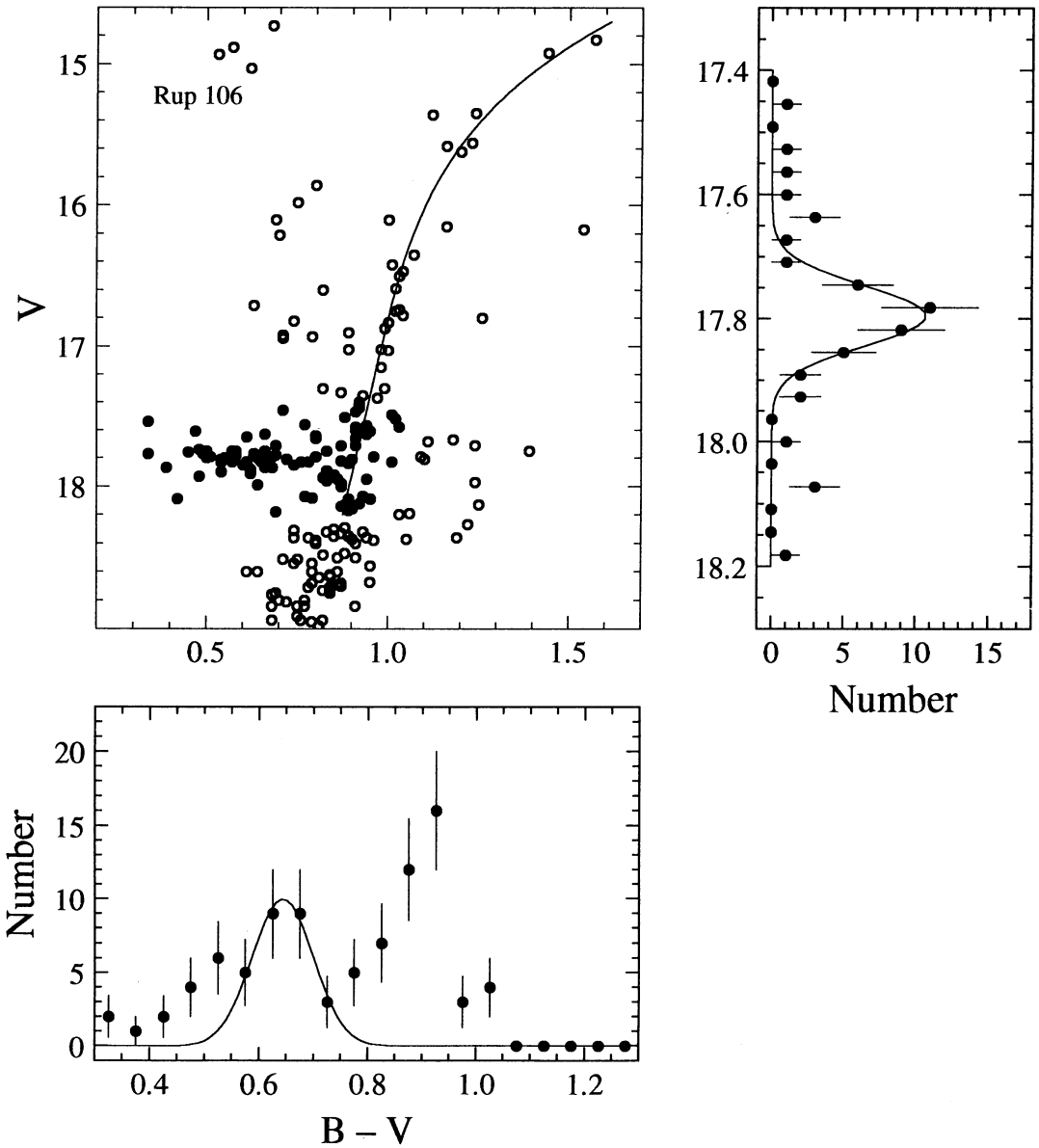

FIG. 3.—Same as Fig. 2, except that the photometry of Rup 106 from Buonanno et al. (1993) is shown

West (1984), while that of Pal 12 is based on the *VI* photometry of Da Costa & Armandroff (1990). The Zinn and West abundance for Pal 12 agrees, to within the errors, with that of Da Costa and Armandroff but has a larger error.

3. THEORETICAL MODELS

In order to compare the observational data for d_{B-V} with the theoretical population models, synthetic HB models were constructed under different assumptions regarding the age and [Fe/H]. The reader is referred to Lee et al. (1990, 1994) for details of the model construction. These HB models were constructed from the HB evolutionary tracks of Lee et al. (1990), and the colors of the RGB were estimated from the Revised Yale Isochrones (Green et al. 1987). The calibration of the theoretical calculations for d_{B-V} was based on the observational data for the globular cluster 47 Tuc. In particular, the HB models have been constructed so that they yield 13 Gyr for the age of 47 Tuc at [Fe/H] $= -0.71$, $\langle (B-V)_o \rangle_{HB} = 0.760$, and $E(B-V) = 0.04$ (see Table 1). The colors of the RGB as estimated from the Revised Yale Isochrones (for $Y = 0.23$) were slightly too red by 0.05 in $B-V$ at the level of the HB. Consequently, the theoretical calculations for d_{B-V} were shifted accordingly so that they reproduce the observational data for 47 Tuc (i.e., $d_{B-V} = 0.196$ at [Fe/H] $= -0.71$). The behavior of d_{B-V} as a function of age and [Fe/H] is illustrated in Figure 4 by the dashed lines. These are plotted in units of 1 Gyr with the youngest age being 7 Gyr (*leftmost dashed line*) and the oldest being 15 Gyr. The model calculations indicate that this variation in d_{B-V} with age is mostly due to the variation of mean HB color with age (see Fig. 6 of Lee 1992), and the color of the RGB at the level of the HB is rather insensitive to age when [Fe/H] < -0.7. These ages represent the case in which the amount of mass loss on the giant branch is fixed and does not vary with age. Note, however, that the HB models incorporating the results of Reimers's (1977) mass-loss relation would show a stronger age dependence (see Figs. 2 and 3 of Lee

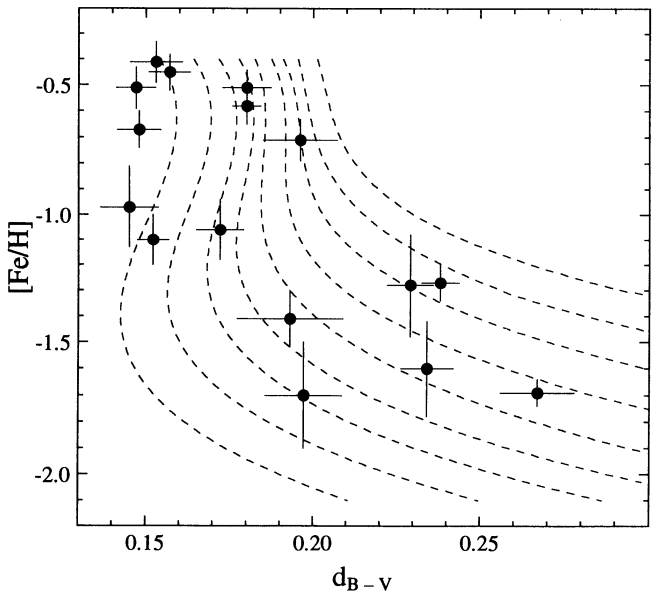

FIG. 4.—Observed variation of d_{B-V} with [Fe/H] for the 16 globular clusters shown in Table 1. The dashed lines represent the predictions of our synthetic horizontal branch models plotted in units of 1 Gyr with the youngest age being 7 Gyr (*leftmost line*) and the oldest being 15 Gyr. Note that these models are calibrated to produce the d_{B-V} value of 47 Tuc at [Fe/H] = −0.71 and an age of 13 Gyr.

et al. 1994). In this case, d_{B-V} would be more sensitive to age than the model's presented here (about two-thirds of the age difference is required to produce a given difference in d_{B-V}).

4. AGES FROM d_{B-V}

The observational data of Table 1 are plotted in Figure 4. Note that, as discussed in the previous section, the models have been constructed so that they yield 13 Gyr for 47 Tuc, which is at [Fe/H] = −0.71 and $d_{B-V} = 0.196$. For each cluster, the values of [Fe/H] and d_{B-V} are used to compute the age based on the grid of theoretical values plotted in Figure 4. In addition, the errors in these quantities are propagated through the calculation by computing the variation in age caused by the uncertainty in [Fe/H] [$\sigma_{[Fe/H]}$(age)] and by the uncertainty in d_{B-V} [$\sigma_{d_{B-V}}$(age)]. The final error in the age is then equal to

$$\sqrt{\sigma_{[Fe/H]}(\text{age})^2 + \sigma_{d_{B-V}}(\text{age})^2}\ .$$

Once the age of each cluster has been calculated, we can use the synthetic HB models to predict the absolute magnitude of the HB [M_V(HB)] given the metallicity and the age. The resultant quantities are plotted in Figure 5, where the dashed lines represent the behavior of M_V(HB) with [Fe/H] for ages ranging from 7 Gyr (*top line*) to 15 Gyr (*bottom line*) in units of 2 Gyr. The errors in M_V(HB) have been computed by propagating the uncertainties in [Fe/H] and age using the method described in the previous paragraph. For comparison, the solid line represents M_V(RR) = 0.17[Fe/H] + 0.79 from Lee (1990). All of the results discussed in this section are summarized in Table 2. Five clusters in our data set, NGC 5927, 6496, 6352, 6366, and ESO 121–SC 03, have d_{B-V}-values that are either close to the edge or outside the grid of theoretical values. For this reason, the ages and M_V(HB)-values for these objects are necessarily more uncertain than the interpolated ones. We note, in passing, that if the HB rectangle of AM-1 included all HB stars shown in the lower right panel of Figure 1, the

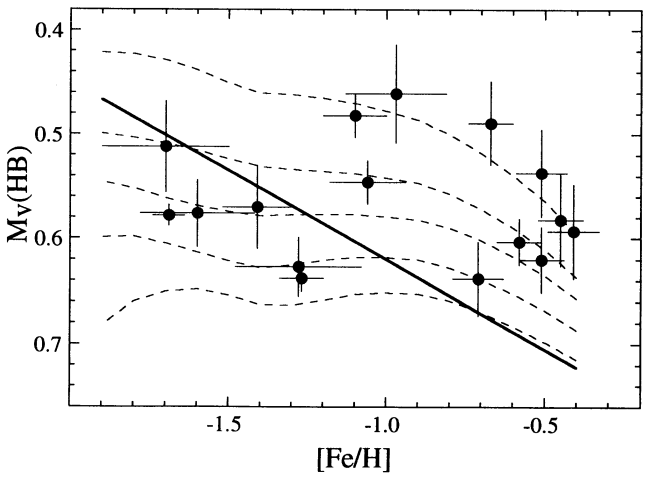

FIG. 5.—Behavior of the derived absolute magnitude of the red horizontal branch [M_V(HB), shown in Table 2] with cluster [Fe/H]. The dashed lines indicate the results of the synthetic horizontal branch models with ages ranging from 7 Gyr (*top line*) to 15 Gyr (*bottom line*) in units of 2 Gyr. From these, the values of M_V(HB) are determined given the age and [Fe/H] of each cluster. The solid line is the relation between M_V(RR) and [Fe/H] from Lee 1990.

derived age of AM-1 would be 10.3 ± 1.4, which, to within the errors, is the same as the value given in Table 2.

5. MAIN-SEQUENCE TURNOFF RESULTS

The majority of the clusters in our sample possess photometry of the main-sequence turnoff. Although there is a great deal of scatter in the CMDs near the turnoff, it is possible to test our relative ages using these data. Figures 6–12 show the deep photometry for NGC 6352, 6366, ESO 121–SC 03, Lindsay 1, Pal 4, Eridanus, and Pal 14, respectively. The photometry is identical to that plotted in Figure 1. Note that we have plotted the Eridanus photometry of Da Costa (1985) as crosses in Figure 11, and, in the case of Pal 14, Figure 12 shows only the data obtained as part of this investigation. The data of Holland & Harris (1992) are not appropriate for the present analysis. In each figure, we have also plotted the fiducial sequence of a standard cluster with a similar metallicity; these are 47 Tuc (Hesser et al. 1987), Pal 12 (Stetson et al. 1989), NGC 362 (Harris 1982; VandenBerg, Bolte, & Stetson 1990), and Rup 106 (Buonanno et al. 1993). The standard clusters

TABLE 2

DERIVED CLUSTER AGES

Name	age (Gyr)	σ	M_V(HB)	σ
NGC 5927	7.0	...	0.59	...
NGC 6496	7.1	...	0.58	...
NGC 6352	6.1	...	0.54	...
NGC 6624	9.9	1.5	0.62	0.03
NGC 6637	9.7	0.9	0.60	0.02
NGC 6366	5.7	...	0.48	...
47 Tuc	13.0	2.1	0.64	0.04
ESO 121–SC 03	6.4	...	0.46	...
Pal 12	9.4	0.8	0.55	0.02
Lindsay 1	7.3	0.6	0.48	0.02
NGC 362	13.6	0.6	0.64	0.01
Pal 4	13.1	1.4	0.63	0.03
Eridanus	10.5	1.0	0.57	0.04
Pal 14	11.2	1.2	0.58	0.03
AM-1	9.2	1.3	0.51	0.04
Rup 106	11.6	0.4	0.58	0.01

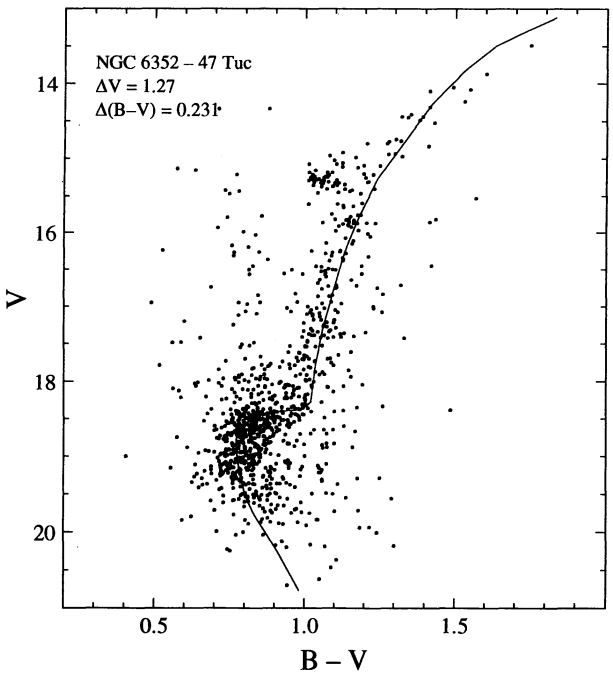

FIG. 6.—Color–magnitude diagram comparison between the photometry of NGC 6352 from Sarajedini & Norris (1994) and the fiducial sequence of 47 Tuc from Hesser et al. (1987). The adopted magnitude and color offsets are specified in the figure and their determination is discussed in the text.

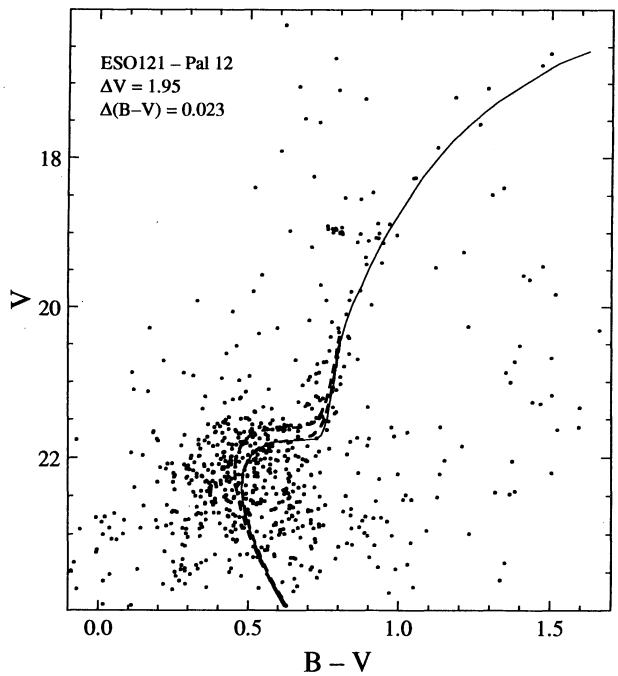

FIG. 8.—Same as Fig. 7, except that the comparison is between the photometry of ESO 121–SC 03 from Mateo et al. (1986) and the fiducial sequence of Pal 12 from Stetson et al. (1989). The isochrones have [Fe/H] = −1.17.

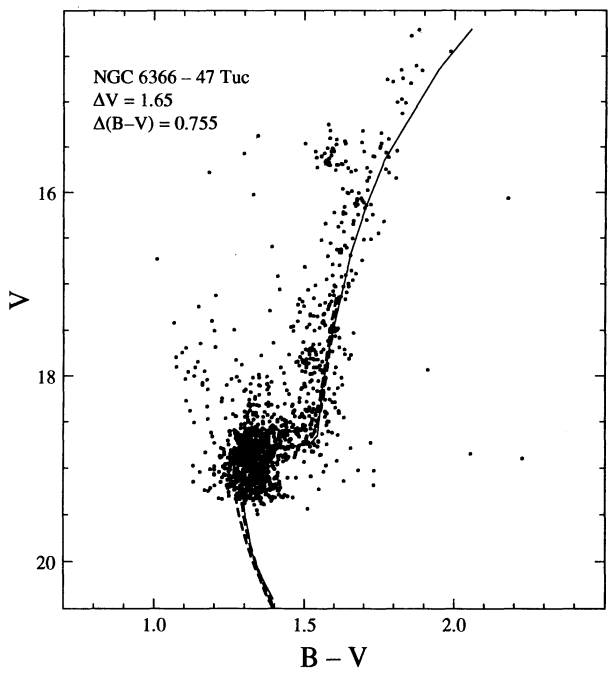

FIG. 7.—Same as Fig. 6, except that the comparison is between the NGC 6366 photometry of Harris (1993) and the 47 Tuc fiducial sequence. The dashed lines are Straniero & Chieffi (1991) isochrones for [Fe/H] = −0.74 illustrating an age difference of 2 Gyr.

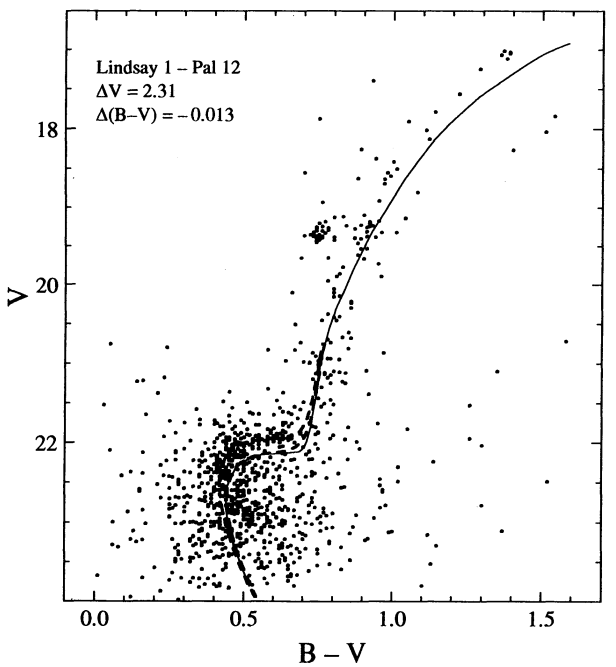

FIG. 9.—Same as Fig. 7, except that the comparison is between the Lindsay 1 photometry of Olszewski et al. (1987) and the Pal 12 fiducial sequence. The isochrones have [Fe/H] = −1.17.

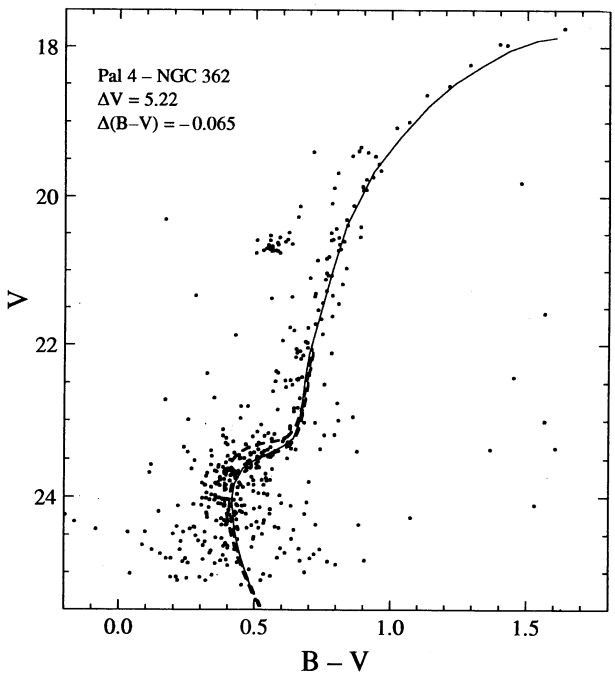

FIG. 10.—Same as Fig. 7, except that the comparison is between the photometry of Pal 4 from Christian & Heasley (1986) and the fiducial sequence of NGC 362 from Harris (1982) and VandenBerg et al. (1990). The isochrones have [Fe/H] = −1.44.

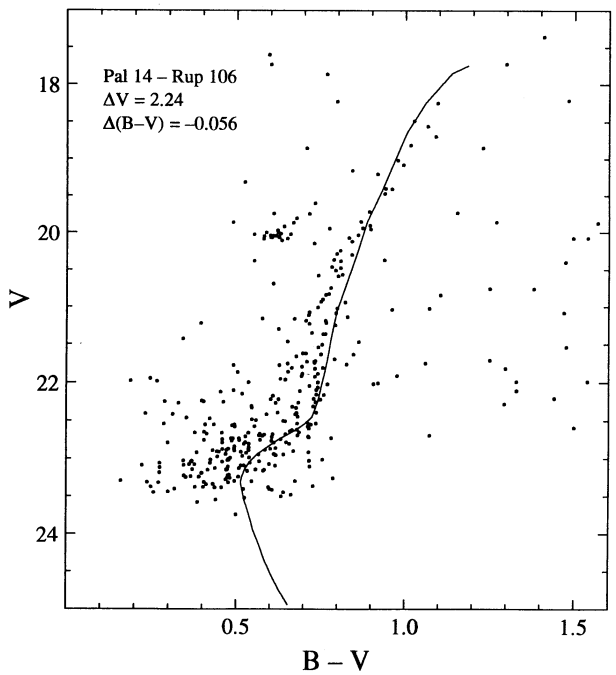

FIG. 12.—Same as Fig. 6, except that the comparison is between the photometry of Pal 14 from the present work and the fiducial sequence of Rup 106 from Buonanno et al. (1993).

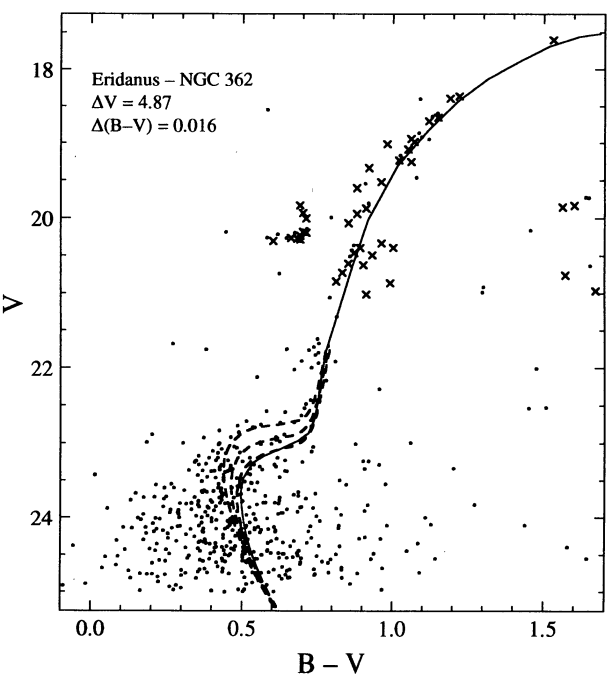

FIG. 11.—Same as Fig. 7, except that the comparison is between the photometry of Eridanus from Da Costa (1985, *crosses*) and Ortolani & Gratton (1989, *points*) and the fiducial sequence of NGC 362 from Harris (1982) and VandenBerg et al. (1990). The isochrones have [Fe/H] = −1.44.

have been shifted in V by the difference in V(HB) and in M_V(HB) that results from a difference in age (Table 2). They have also been shifted in $B-V$ by the difference in $(B-V)_g$ plus 0.01 mag for each 3 Gyr age difference (see Da Costa, Armandroff, & Norris 1992). The resulting offsets are given in each figure.

To interpret the relative locations of the turnoffs in terms of an age difference, we use the isochrones of Straniero & Chieffi (1991) at the appropriate metallicity. For the standard clusters, these are [Fe/H] = −0.74 for 47 Tuc, [Fe/H] = −1.17 for Pal 12, and [Fe/H] = −1.44 for NGC 362. Straniero & Chieffi used very similar values in their isochrone fits to these clusters. Guided by the ages derived from these fits, our strategy is to reproduce the shape of the principal sequence of each standard cluster by applying arbitrary shifts to the isochrones in the color-magnitude plane. We are then interested in estimating the age of the cluster in question relative to the standard cluster using isochrones of various ages that have had the same shifts applied to them. All of the isochrones plotted in a certain figure differ in age by 2 Gyr. No isochrones are plotted in Figures 6 and 12 because the clusters being compared appear to have approximately the same age. By examining Figures 6–12, we estimate the relative ages listed in Table 3. These are given in the sense (cluster − standard). It should be pointed out that the precision of these ages is only $\approx \pm 2$ Gyr. Table 3 also lists the relative ages as yielded by d_{B-V} from Table 2. Finally, the last column of Table 3 gives the difference between these two methods. Keeping in mind that the d_{B-V} age diagnostic yields a reasonable age of 13 Gyr for 47 Tuc, Table 3 indicates that d_{B-V}, as calibrated using the theoretical models presented here, breaks down for clusters with [Fe/H] > −0.7. This is not surprising; Figure 4 shows that d_{B-V} looses much of

TABLE 3

COMPARISON OF RELATIVE CLUSTER AGES

Cluster	[Fe/H]	Standard	[Fe/H]	Δ age (MSTO)	Δ age (d_{B-V})	Difference
NGC 6352	−0.51	47 Tuc	−0.71	0	−6.9	6.9
NGC 6366	−0.67	47 Tuc	−0.71	−2	−7.2	5.2
ESO 121–SC 03	−0.93	Pal 12	−1.06	−2	−3.0	1.0
Lindsay 1	−1.10	Pal 12	−1.06	−2	−1.8	−0.2
Pal 4	−1.28	NGC 362	−1.27	−1	−0.5	−0.5
Eridanus	−1.41	NGC 362	−1.27	−3	−3.1	0.1
Pal 14	−1.60	Rup 106	−1.69	0	−0.4	0.4

its age sensitivity for clusters with [Fe/H] > −0.7.[2] As a result, for the remainder of this discussion, we will ignore these clusters.

6. DISCUSSION

It is interesting to combine the ages derived herein with those of Chaboyer et al. (1992, hereafter CSD)[3], which are determined via the ΔV (magnitude difference between the RR Lyrae variables and the main-sequence turnoff) method. To do this, we must determine any zero point offset between these two sets of ages. First, we correct the ΔV ages of red HB clusters using the M_V(HB) values in Table 2 to account for the fact that few if any RR Lyraes exist in these clusters. This procedure produces the following revised ΔV ages: 13.5 ± 2.8 Gyr for 47 Tuc, 10.0 ± 1.4 Gyr for Pal 12, 11.3 ± 1.6 Gyr for NGC 362, and 9.6 ± 0.9 Gyr for Rup 106. The mean difference between these ages and the d_{B-V} ages [age(ΔV) − age(d_{B-V})] is −0.8 ± 0.7 Gyr, which is not statistically significant. As a result, we will combine the two sets of ages without applying any kind of zero point correction. For clusters in common, we adopt the d_{B-V} age.

Figure 13 shows the age–metallicity relation for the combined set of cluster ages. The circles represent the ΔV ages of CSD, while the squares are the d_{B-V} ages derived herein. The filled symbols are clusters inside 8 kpc of the Galactic center, and the open symbols are those outside 8 kpc. The solid and dashed lines are the weighted least-squares fits to the clusters inside and outside 8 kpc, respectively. In Figure 14, we show the variation of age with the logarithm of the Galactocentric distance (R_{GC}), wherein the dashed line indicates 8 kpc. As pointed out by CSD and Lee et al. (1994), these two figures show that the age spread among the inner halo clusters is relatively small, whereas among the outer halo clusters there is a significant range in ages. The outer halo clusters added by the d_{B-V} method reinforce these conclusions.

The age spread at constant metallicity, which is illustrated in Figure 13, is the so-called second parameter effect. Several authors have argued that age is the dominant second parameter among the Galactic globular clusters (Sarajedini & King 1989; Green & Norris 1990; CSD; Lee, Demarque, & Zinn 1988, 1994). The present study shows that the Galactic globu-

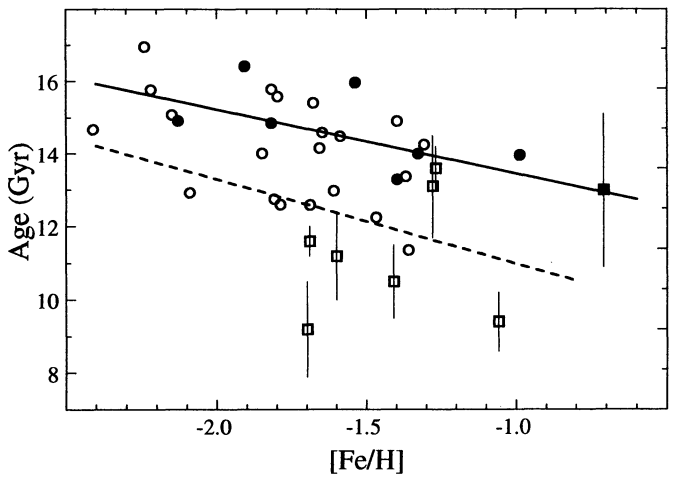

FIG. 13.—Observed relation between age and metallicity for globular clusters with Galactocentric distances less than 8 kpc (*filled symbols*) and greater than 8 kpc (*open symbols*). The circles represent ages derived by Chaboyer et al. (1992) using the magnitude difference between the main-sequence turnoff and the horizontal branch, while the squares are ages yielded by d_{B-V}. The solid line represents a weighted fit to the filled symbols, while the dashed line is a weighted fit to the open symbols.

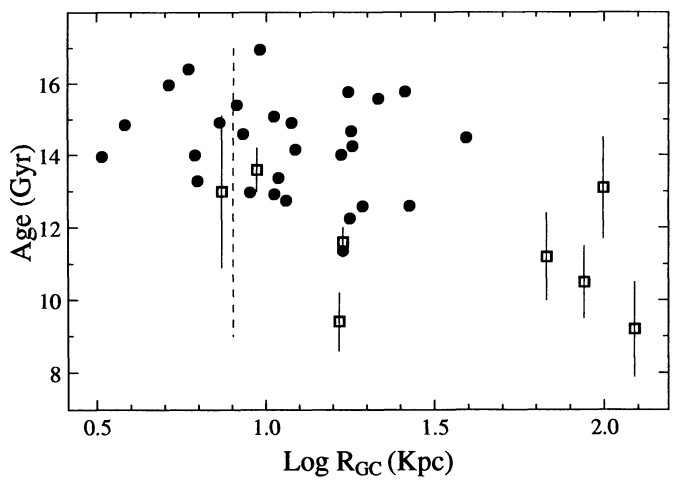

FIG. 14.—Observed relation between age and Galactocentric distance (R_{GC}) for globular clusters with ages derived by Chaboyer et al. (1992) using the magnitude difference between the main-sequence turnoff and the horizontal branch (*filled circles*) and those with ages yielded by d_{B-V} (*open squares*). The vertical dashed line has been placed at 8 kpc.

[2] It is important to point out that this loss of age sensitivity is not related to the fact that we have calibrated our theoretical d_{B-V} values to 47 Tuc. We could have chosen NGC 362 or Pal 12; their d_{B-V} ages are in reasonable accord with their turnoff ages. We selected 47 Tuc because its properties (metal abundance, reddening, age, etc.) are known with more confidence than those of NGC 362 and Pal 12.

[3] Note that the difference between the ages published by Chaboyer et al. (1992) and Chaboyer et al. (1995) is negligible, indicating that the results of the present analysis would remain unchanged if the latter data set were used.

lar clusters with $(B-R)/(B+V+R) < -0.80$ (i.e., red HB clusters) have a weighted mean age of $\langle age \rangle = 11.6 \pm 0.3$ Gyr, where the uncertainty is the standard error of the weighted mean. In contrast, the clusters with $(B-R)/(B+V+R) > -0.80$ from the study of CSD (excluding Palomar 13 because of its uncertain HB morphology) have $\langle age \rangle = 14.0 \pm 0.3$ Gyr, leading to the conclusion that the red HB clusters are younger than the remaining clusters by 2.4 ± 0.4 Gyr. If, instead, we divide this data set, via the prescription of Zinn (1993; see also Da Costa & Armandroff 1995) into a "younger halo" group and an "old halo" group, we find that the former has $\langle age \rangle = 11.9 \pm 0.2$ Gyr, whereas the latter has $\langle age \rangle = 14.6 \pm 0.5$ Gyr, leading to a difference of 2.7 ± 0.5 Gyr.

CSD examined the variation of age as a function of HB morphology for clusters in a small range of metallicity, i.e., $-1.75 \leq [Fe/H] \leq -1.25$. They found that clusters with blue HBs are significantly older than clusters with red HBs, thereby lending credence to the notion that age is the dominant second parameter. However, they did not include any clusters with purely red HBs in their analysis. They did have a ΔV age for Pal 12, but its [Fe/H] is greater than -1.25. Since we now have ages for red HB clusters with abundances in the range $-1.75 \leq [Fe/H] \leq -1.25$, it is possible to combine these with the CSD ΔV ages. In order to take full advantage of the most internally consistent ΔV data, we limit ourselves to ages derived from photometry published by Buonanno, Corsi, & Fusi Pecci (1989), Buonanno et al. (1991), and Buonanno et al. (1993), collectively referred to as BCF in Table 3 of CSD. Figure 15 shows the variation of age with HB morphology as quantified by $(B-R)/(B+V+R)$. The circles are the ΔV ages and the squares are the d_{B-V} ages. The solid line is the weighted least squares fit to these data and is significant at greater than the 99.9% confidence level. This reinforces the conclusions of Lee et al. (1988, 1994), CSD, and others that age is the second parameter, which, in addition to metal abundance, governs the morphology of the HB.

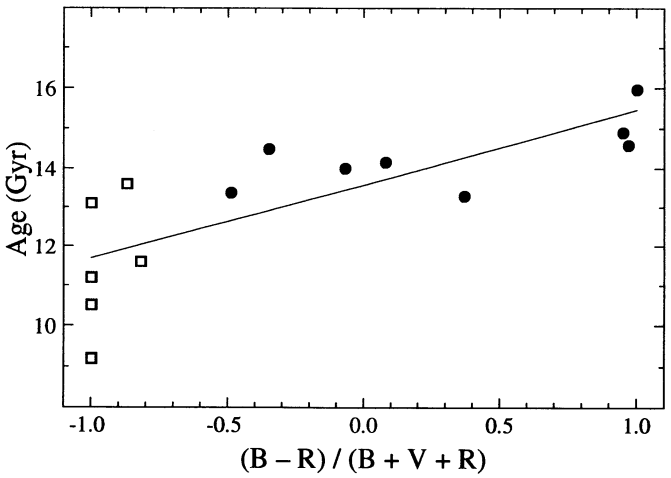

FIG. 15.—Observed relation between age and horizontal branch morphology, $(B-R)/(B+V+R)$ (see text), for globular clusters with $-1.75 \leq [Fe/H] \leq -1.25$. The filled circles are the ages from Chaboyer et al. (1992) using the magnitude difference between the main-sequence turnoff and the horizontal branch. The open squares are the ages derived herein via d_{B-V}. The solid line is the weighted least-squares fit to these data. The slope of this line is significant at more than the 99.9% level.

We are grateful to Ed Olszewski for providing the photometry of Lindsay 1, Stephen Holland for providing Pal 14, Carlo Corsi for providing Rup 106, and Taft Armandroff for useful suggestions that greatly improved this work. Y. W. L. acknowledges support from the Korean Ministry of Education (project No. BSRI-94-5413).

REFERENCES

Armandroff, T. E., & Da Costa, G. S. 1991, AJ, 101, 1329
Armandroff, T. E., Da Costa, G. S., & Zinn, R. J. 1992, AJ, 104, 164
Buonanno, R., Buscema, G., Corsi, C. E., & Iannicola, G. 1983, A&AS, 51, 83
Buonanno, R., Corsi, C. E., & Fusi Pecci, F. 1985, A&A, 145, 97
———. 1989, A&A, 216, 80
Buonanno, R., Corsi, C. E., Fusi Pecci, F., Richer, H. B., & Fahlman, G. G. 1993, AJ, 105, 184
Buonanno, R., Fusi Pecci, F., Capellaro, E., Ortolani, S., Richtler, T., & Geyer, E. H. 1991, AJ, 102, 1005
Buzzoni, A., Fusi Pecci, F., Buonanno, R., & Corsi, C. E. 1983, A&A, 128, 94
Chaboyer, B., Sarajedini, A., & Demarque, P. 1992, ApJ, 394, 515 (CSD)
———. 1995, in preparation
Christian, C. A., & Heasley, J. N. 1986, ApJ, 303, 216
Da Costa, G. S. 1985, ApJ, 291, 230
Da Costa, G. S., & Armandroff, T. E. 1990, AJ, 100, 162
———. 1995, AJ, in press
Da Costa, G. S., Armandroff, T. E., & Norris, J. E. 1992, AJ, 104, 154
Da Costa, G. S., & Hatzidimitriou, D. 1995, in preparation
Djorgovski, S. G. 1993, in The Structure and Dynamics of Globular Clusters, ed. S. G. Djorgovski & G. Meylan (San Francisco: ASP), 373
Ferraro. F., Clementini, G., Fusi Pecci, F., Sortino, R., & Buonanno, R. 1992, MNRAS, 256, 391
Green, E. M., & Norris, J. E. 1990, ApJ, 353, L17
Green, E. M., Demarque, P., & King, C. R. 1987, The Revised Yale Isochrones and Luminosity Functions (New Haven: Yale Univ. Obs.)
Harris, H. C. 1993, AJ, 106, 604
Harris, W. E. 1982, ApJS, 50, 573
Hatzidimitriou, D. 1991, MNRAS, 251, 545
Hesser, J. E., Harris, W. E., VandenBerg, D. A., Allwright, J. W. B., Shott, P., & Stetson, P. B. 1987, PASP, 99, 739
Holland, S., & Harris, W. E. 1992, AJ, 103, 131
Iben, I., Jr. 1968, Nature, 220, 143
Keeping, E. S. 1962, Introduction to Statistical Inference (Princeton: Van Nostrand)
Landolt, A. U. 1992, AJ, 104, 340
Lee, Y. W. 1990, ApJ, 363, 159
———. 1992, AJ, 104, 1780
Lee, Y. W., Demarque, P., & Zinn, R. 1988, in Calibration of Stellar Ages, ed. A. G. D. Davis Philip (Schenectady: Davis), 141
———. 1990, ApJ, 350, 155
———. 1994, ApJ, 423, 248
Madore, B. F., & Freedman, W. L. 1989, ApJ, 340, 812
Mateo, M., Hodge, P., & Schommer, R. A. 1986, ApJ, 311, 113
Olszewski, E. W., Schommer, R. A., & Aaronson, M. 1987, AJ, 93, 565
Olszewski, E. W., Schommer, R. A., Suntzeff, N. B., & Harris, H. C. 1991, AJ, 101, 515
Ortolani, S., & Gratton, R. G. 1989, A&AS, 79, 155
Pryor, C., & Meylan, G. 1993, in The Structure and Dynamics of Globular Clusters, ed. S. G. Djorgovski & G. Meylan (San Francisco: ASP), 357
Reimers, D. 1977, A&A, 57, 395
Sarajedini, A. 1994, PASP, 106, 404
Sarajedini, A., & Da Costa, G. S. 1991, AJ, 102, 628
Sarajedini, A., & King, C. R. 1989, AJ, 98, 1624
Sarajedini, A., & Norris, J. E. 1994, ApJS, 93, 161
Stetson, P. B. 1987, PASP, 99, 191
Stetson, P. B., VandenBerg, D. A., Bolte, M., Hesser, J. E., & Smith, G. H. 1989, AJ, 97, 1360
Straniero, O., & Chieffi, A. 1991, ApJS, 76, 525
Suntzeff, N. B., Kraft, R. P., & Kinman, T. D. 1988, AJ, 95, 91
Suntzeff, N. B., Olszewski, E., & Stetson, P. B. 1985, AJ, 90, 1481
Trager, S. C., Djorgovski, S., & King, I. R. 1993, in The Structure and Dynamics of Globular Clusters, ed. S. G. Djorgovski & G. Meylan (San Francisco: ASP), 347
VandenBerg, D. A., Bolte, M., & Stetson, P. B. 1990, AJ, 100, 445
Zinn, R. J. 1993, in The Globular Cluster–Galaxy Connection, ed. G. Smith & J. Brodie (San Francisco: ASP), 38
Zinn, R. J., & West, M. J. 1984, ApJS, 55, 45